Supplementary Information

Transcription regulation of African swine fever virus: dual role of M1249L

Dongming Zhao, Nan Wang, Xiaoying Feng, Zhenjiang Zhang, Kongen Xu, Tao Zheng, Yunge Yang, Xuemei Li, Xianjin Ou, Rui Zhao, Zihe Rao, Zhigao Bu, Yutao Chen, Xiangxi Wang

Corresponding author: raozh@ibp.ac.cn；buzhigao@caas.cn；chenyutao@ibp.ac.cn；xiangxi@ibp.ac.cn

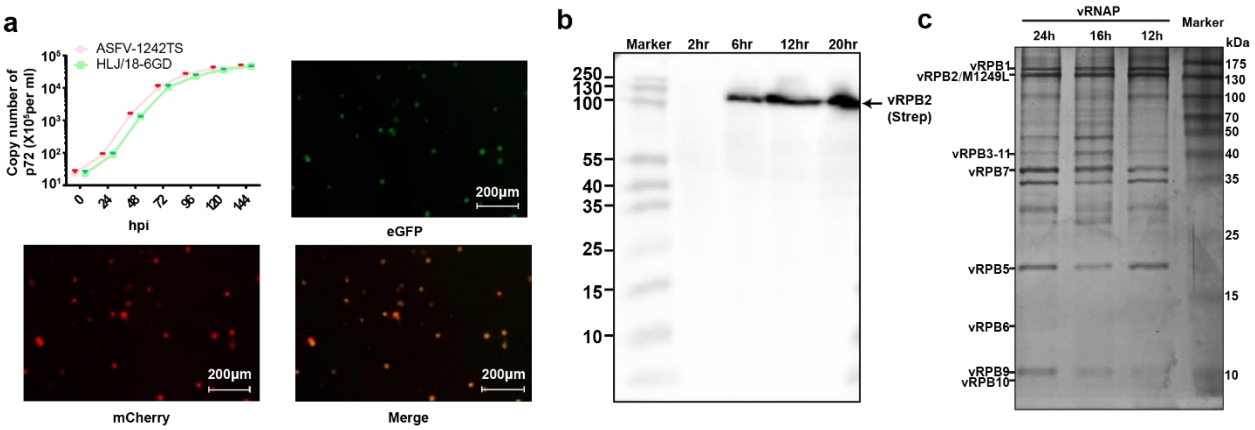

Supplementary Figure 1: Purification and Activity of ASFV vRNAP-M1249L Complexes.

(**a**) Replication of ASFV-1242TS in comparison to its parental virus HLJ/18-6GD. Virus titer was determined for the indicated time points from infected cells and cell culture supernatant, respectively. Fluorescence of eGFP and mCherry indicate the recombinant virus construct is successfully accomplished. (**b**) Western blot analysis for monitoring protein expression at different time points. (**c**) Proteins eluted from XT beads at different time points visualized by silver staining on a 12.5% SDS-PAGE.

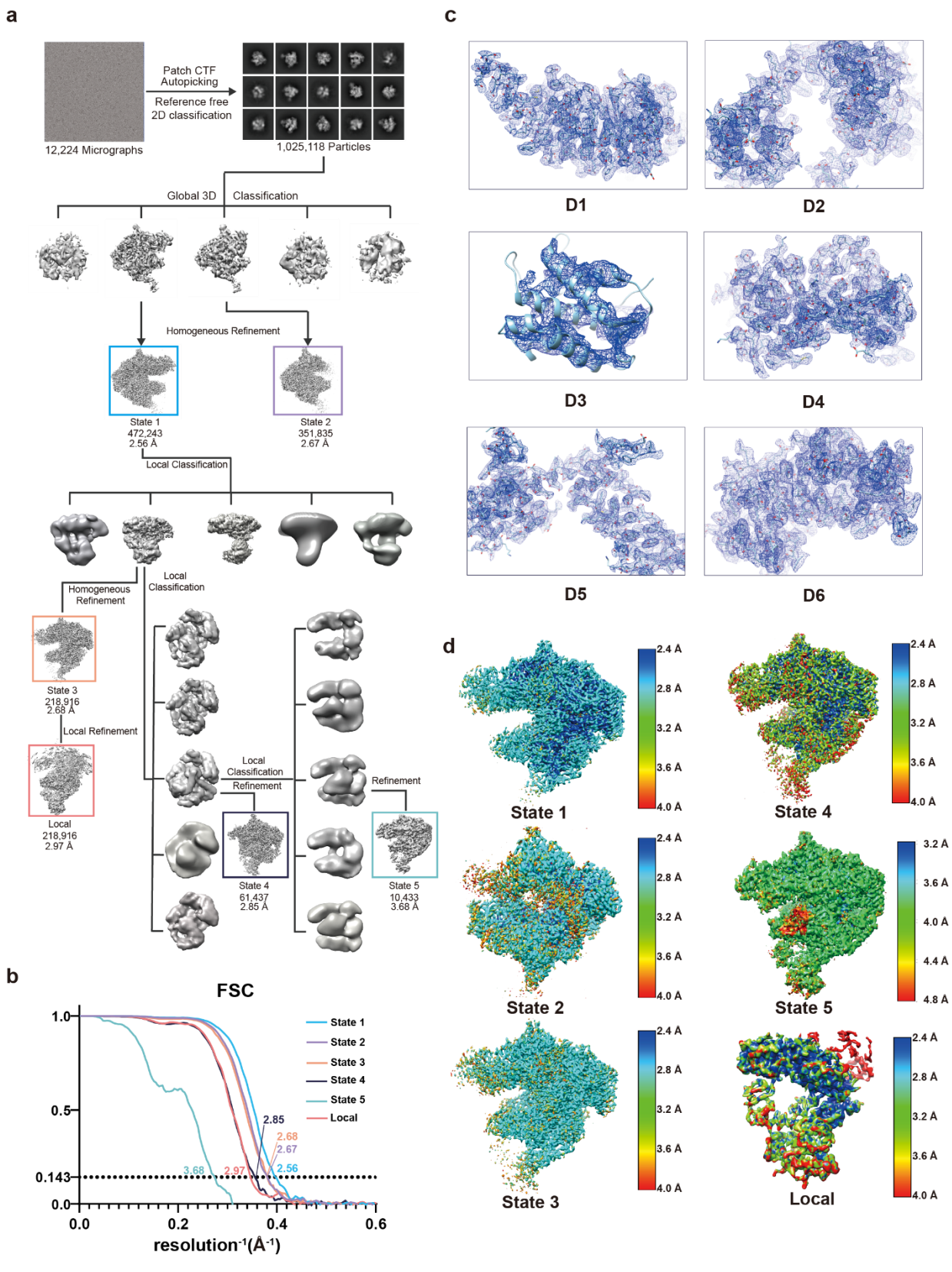
a
Patch CTF Autopicking
Reference free 2D classification
12,224 Micrographs
1,025,118 Particles
Global 3D Classification
Homogeneous Refinement
State 1
472,243
2.56 Å
State 2
351,835
2.67 Å
Local Classification
Homogeneous Refinement
Local Classification
State 3
218,916
2.68 Å
Local Refinement
Local
218,916
2.97 Å
Local Classification
Refinement
Refinement
State 4
61,437
2.85 Å
State 5
10,433
3.68 Å
b
FSC
1.0
0.5
0.143
0.0
0.0
0.2
0.4
0.6
resolution⁻¹(Å⁻¹)
State 1
State 2
State 3
State 4
State 5
Local
2.85
2.68
2.67
2.56
3.68
2.97
c
D1
D2
D3
D4
D5
D6
d
State 1
State 2
State 3
State 4
State 5
Local
2.4 Å
2.8 Å
3.2 Å
3.6 Å
4.0 Å
4.4 Å
4.8 Å

Supplementary Figure 2: Structure Determination of ASFV vRNAP-M1249L Complex. (**a**) Follow chart of image processing. State 1 (PDB: 8YQT, EMD-39505), state 2 (PDB: 8YQV, EMD-39507), state 3 (PDB: 8YQW, EMD-39508), state 4 (PDB: 8YQU, EMD-39506), state 5 (PDB: 8YQY, EMD-39510), local (PDB: 8YQW, EMD-39508). (**b**) FSC plots for consensus refinement. (**c**) Representative density of ASFV M1249L reconstruction. (**d**) Local resolution mapped to the reconstruction density isosurface.

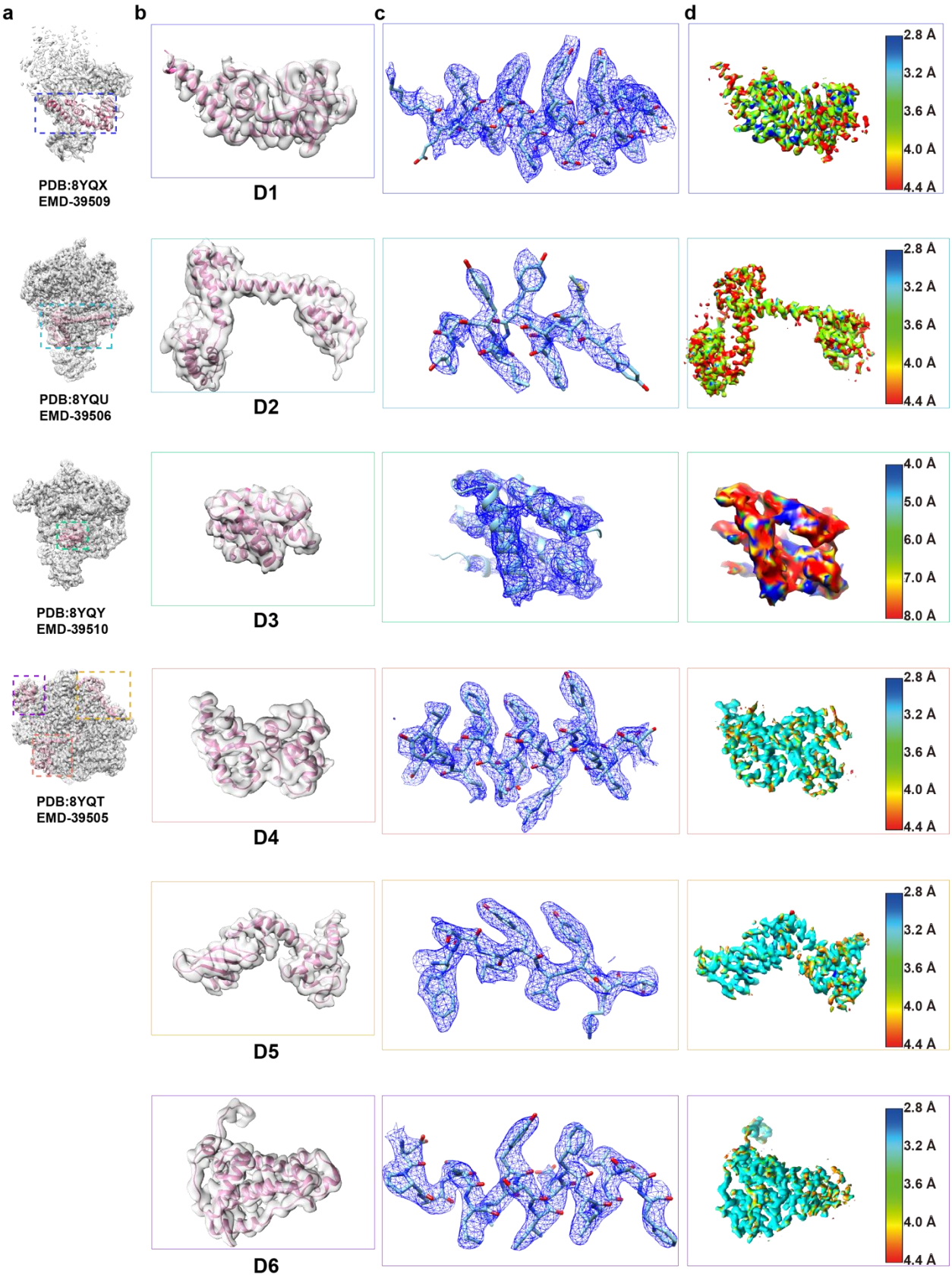
a
b
c
d
PDB:8YQX
EMD-39509
D1
2.8 Å
3.2 Å
3.6 Å
4.0 Å
4.4 Å
PDB:8YQU
EMD-39506
D2
2.8 Å
3.2 Å
3.6 Å
4.0 Å
4.4 Å
PDB:8YQY
EMD-39510
D3
4.0 Å
5.0 Å
6.0 Å
7.0 Å
8.0 Å
PDB:8YQT
EMD-39505
D4
2.8 Å
3.2 Å
3.6 Å
4.0 Å
4.4 Å
D5
2.8 Å
3.2 Å
3.6 Å
4.0 Å
4.4 Å
D6
2.8 Å
3.2 Å
3.6 Å
4.0 Å
4.4 Å

Supplementary Figure 3: Density maps and atomic models of ASFV M1249L.(**a**) Maps used for the reconstruction of various domains of M1249L and the reconstructed pdbs. The cartoon representation of the reconstructed domains of M1249L is displayed in pink and outlined with a dashed box. (**b**) Electron density maps of ASFV M1249L are shown overlaid with the corresponding model. (**c**) Representative density of ASFV M1249L reconstruction. (**d**) Local resolution mapped to the reconstruction density isosurface.

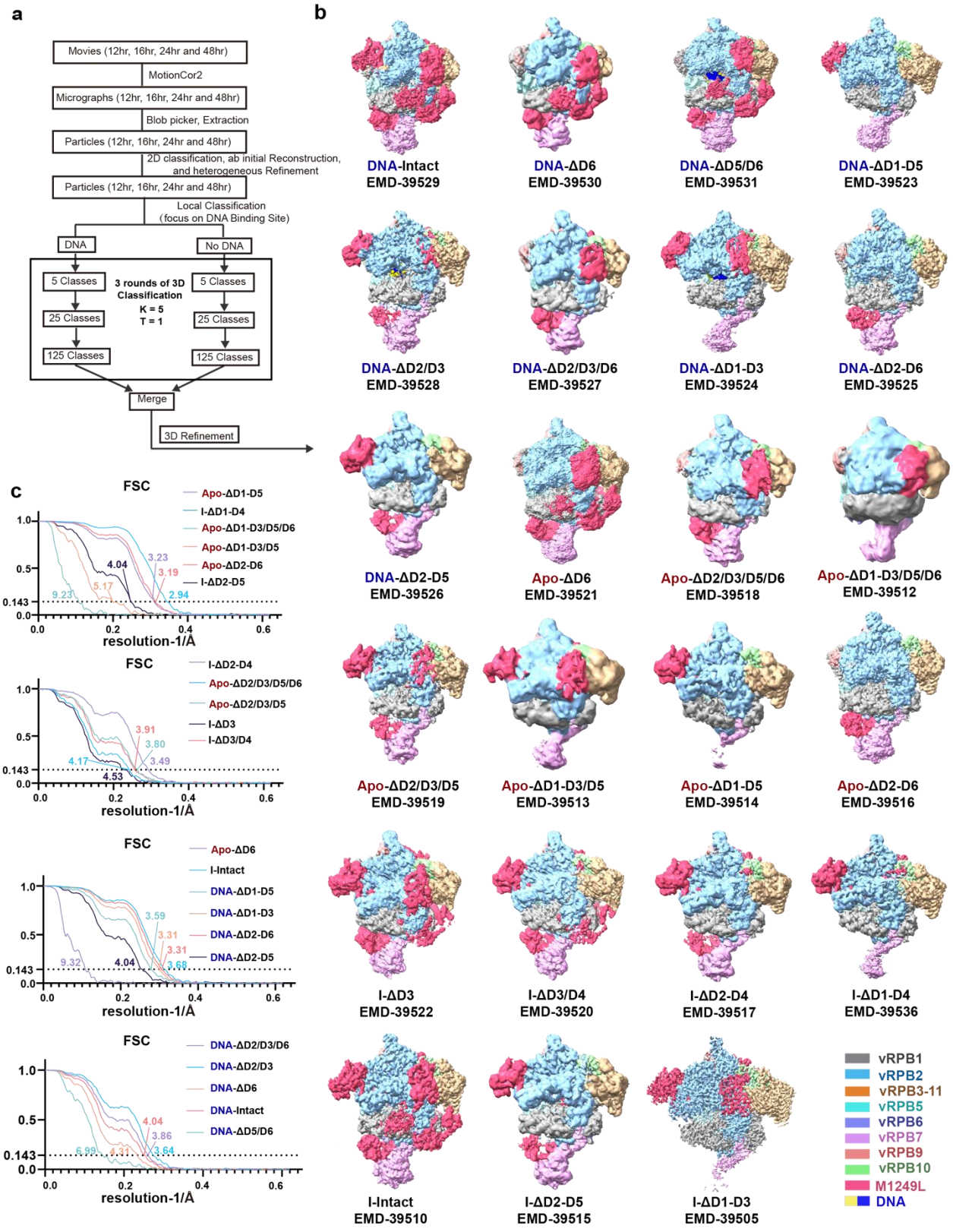
a
Movies (12hr, 16hr, 24hr and 48hr)
MotionCor2
Micrographs (12hr, 16hr, 24hr and 48hr)
Blob picker, Extraction
Particles (12hr, 16hr, 24hr and 48hr)
2D classification, ab initial Reconstruction, and heterogeneous Refinement
Particles (12hr, 16hr, 24hr and 48hr)
Local Classification (focus on DNA Binding Site)
DNA
No DNA
5 Classes
25 Classes
125 Classes
3 rounds of 3D Classification K = 5 T = 1
5 Classes
25 Classes
125 Classes
Merge
3D Refinement
b
DNA-Intact EMD-39529
DNA-ΔD6 EMD-39530
DNA-ΔD5/D6 EMD-39531
DNA-ΔD1-D5 EMD-39523
DNA-ΔD2/D3 EMD-39528
DNA-ΔD2/D3/D6 EMD-39527
DNA-ΔD1-D3 EMD-39524
DNA-ΔD2-D6 EMD-39525
DNA-ΔD2-D5 EMD-39526
Apo-ΔD6 EMD-39521
Apo-ΔD2/D3/D5/D6 EMD-39518
Apo-ΔD1-D3/D5/D6 EMD-39512
Apo-ΔD2/D3/D5 EMD-39519
Apo-ΔD1-D3/D5 EMD-39513
Apo-ΔD1-D5 EMD-39514
Apo-ΔD2-D6 EMD-39516
I-ΔD3 EMD-39522
I-ΔD3/D4 EMD-39520
I-ΔD2-D4 EMD-39517
I-ΔD1-D4 EMD-39536
I-Intact EMD-39510
I-ΔD2-D5 EMD-39515
I-ΔD1-D3 EMD-39505
vRPB1
vRPB2
vRPB3-11
vRPB5
vRPB6
vRPB7
vRPB9
vRPB10
M1249L
DNA
c
FSC
Apo-ΔD1-D5
I-ΔD1-D4
Apo-ΔD1-D3/D5/D6
Apo-ΔD1-D3/D5
Apo-ΔD2-D6
I-ΔD2-D5
4.04
3.23
3.19
5.17
9.23
2.94
resolution-1/Å
FSC
I-ΔD2-D4
Apo-ΔD2/D3/D5/D6
Apo-ΔD2/D3/D5
I-ΔD3
I-ΔD3/D4
3.91
3.80
4.17
3.49
4.53
resolution-1/Å
FSC
Apo-ΔD6
I-Intact
DNA-ΔD1-D5
DNA-ΔD1-D3
DNA-ΔD2-D6
DNA-ΔD2-D5
3.59
3.31
3.31
9.32
4.04
3.68
resolution-1/Å
FSC
DNA-ΔD2/D3/D6
DNA-ΔD2/D3
DNA-ΔD6
DNA-Intact
DNA-ΔD5/D6
4.04
3.86
6.99
4.31
3.64
resolution-1/Å

Supplementary Figure 4: Structure Determination of Dynamic ASFV vRNAP-M1249L Complex. (**a**)Follow chart of image processing. (**b**) The dynamic variations of M1249L are depicted across 23 distinct cryo-EM maps. The color scheme is indicated at the right bottom of the panel. (**c**) FSC plots for consensus refinement.

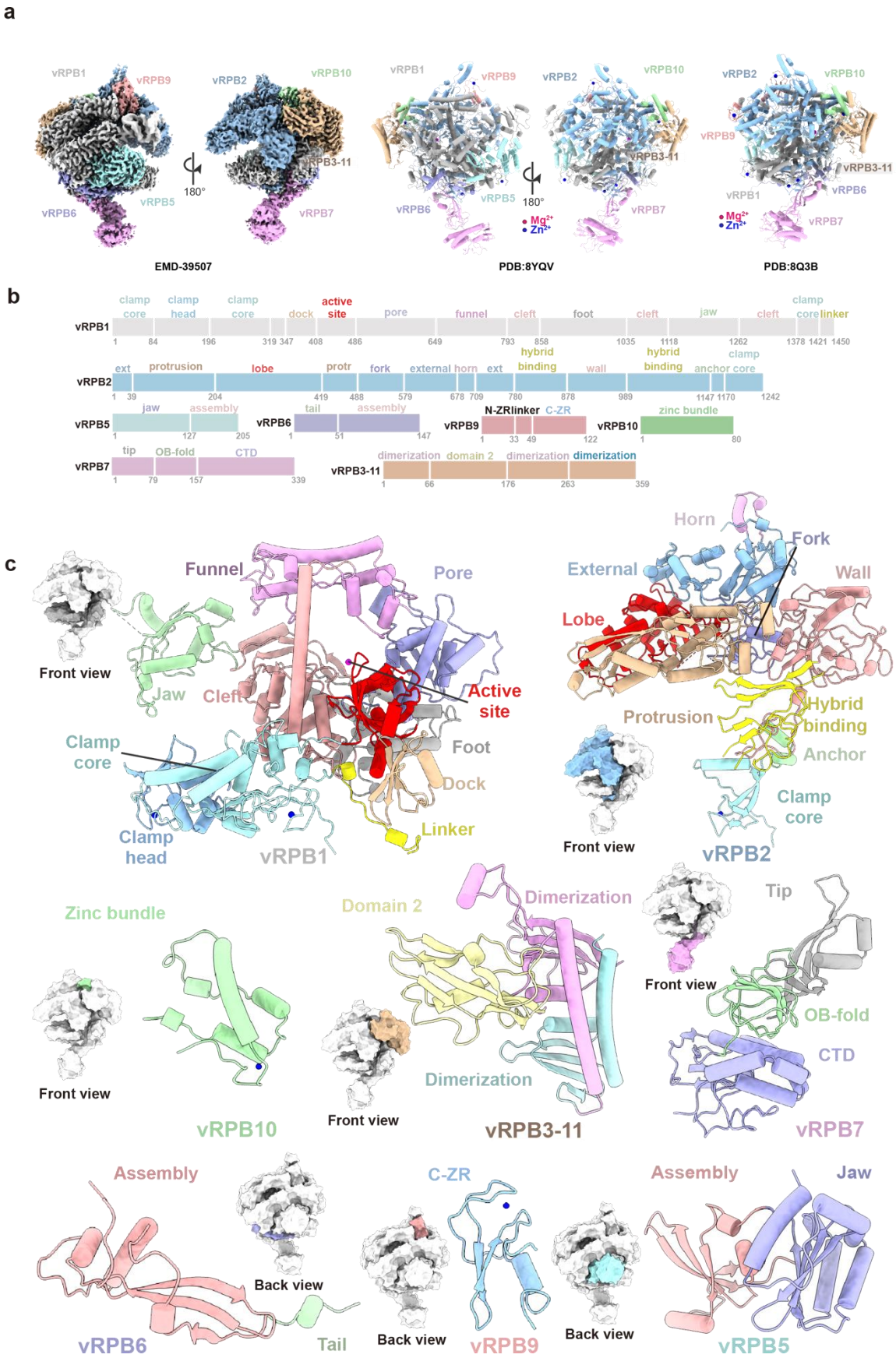
a
vRPB1
vRPB9
vRPB2
vRPB10
vRPB3-11
vRPB5
vRPB6
vRPB7
180°
EMD-39507
PDB:8YQV
PDB:8Q3B
Mg2+
Zn2+
b
vRPB1
clamp core
clamp head
clamp core
dock
active site
pore
funnel
cleft
foot
cleft
jaw
cleft
clamp core
linker
vRPB2
ext
protrusion
lobe
protr
fork
external
horn
ext
hybrid binding
wall
hybrid binding
clamp anchor core
vRPB5
jaw
assembly
vRPB6
tail
assembly
vRPB9
N-ZRlinker
C-ZR
vRPB10
zinc bundle
vRPB7
tip
OB-fold
CTD
vRPB3-11
dimerization
domain 2
dimerization
dimerization
c
Funnel
Pore
Front view
Jaw
Cleft
Active site
Clamp core
Foot
Dock
Linker
Clamp head
vRPB1
Horn
Fork
External
Wall
Lobe
Protrusion
Hybrid binding
Anchor
Clamp core
Front view
vRPB2
Zinc bundle
Front view
vRPB10
Domain 2
Dimerization
Front view
Dimerization
vRPB3-11
Tip
Front view
OB-fold
CTD
vRPB7
Assembly
Back view
vRPB6
Tail
C-ZR
Back view
vRPB9
Back view
Assembly
Jaw
vRPB5

Supplementary Figure 5: ASFV core vRNAP resembles typical eukaryotic RNA polymerase II architecture. (**a**) The cryo-EM map and the structure of the ASFV RNA polymerase core (left, EMD-39507; middle, PDB:8YQV). The protein subunits are shown in cartoon depiction, with helices depicted as cylinders. Comparison of our ASFV RNAP core to the previously reported recombinant insect cell expressed RNAP (left, PDB: 8Q3B). Subunits are colored as in (b). The active site metal Mg^{2+} and bound structural zinc ions are shown as spheres. **(b)** Schematic depiction of ASFV vRNAP subunits. Functional domains are annotated based on structure-based sequence alignment with VACV vRNAP. **(c)** Cartoon depiction of ASFV vRNAP subunits with structural details shown. All subunits are colored as indicated in (b). The location of the subunits in vRNAP complex is indicated schematically.

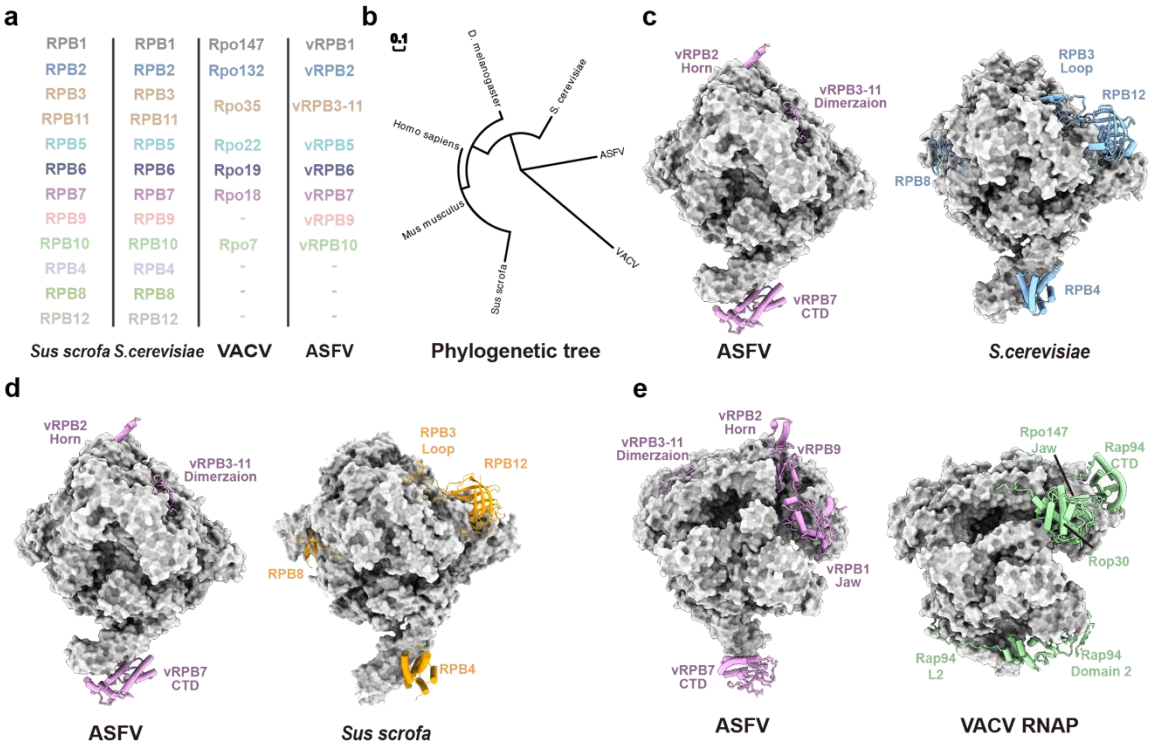

Supplementary Figure 6: Comparation of ASFV RNA polymerase to homolog RNA polymerases. (**a**) Comparison of ASFV RNA Polymerase subunit composition to *S. cerevisiae* Pol II (PDB: 1WCM), Vaccinia RNA Polymerase (PDB: 6RIC), and *Sus scrofa* Pol II (PDB: 7EG7). The enzymes are depicted in schematic surface representation. Homologous subunits are indicated in the table and colored accordingly. (**b**) Phylogenetic tree analysis based on RNA polymerase sequence. (**c/d/e**) Detailed comparison of ASFV vRNAP with the other three RNA polymerases in pairs. The largely conserved core is depicted as schematic surface in gray, and the differing regions are depicted as cartoon. Regions specific to ASFV vRNAP are shown in purple and regions specific to *S. cerevisiae* Pol II in blue, Vaccinia RNA Polymerase in green and *Sus scrofa* Pol II in orange.

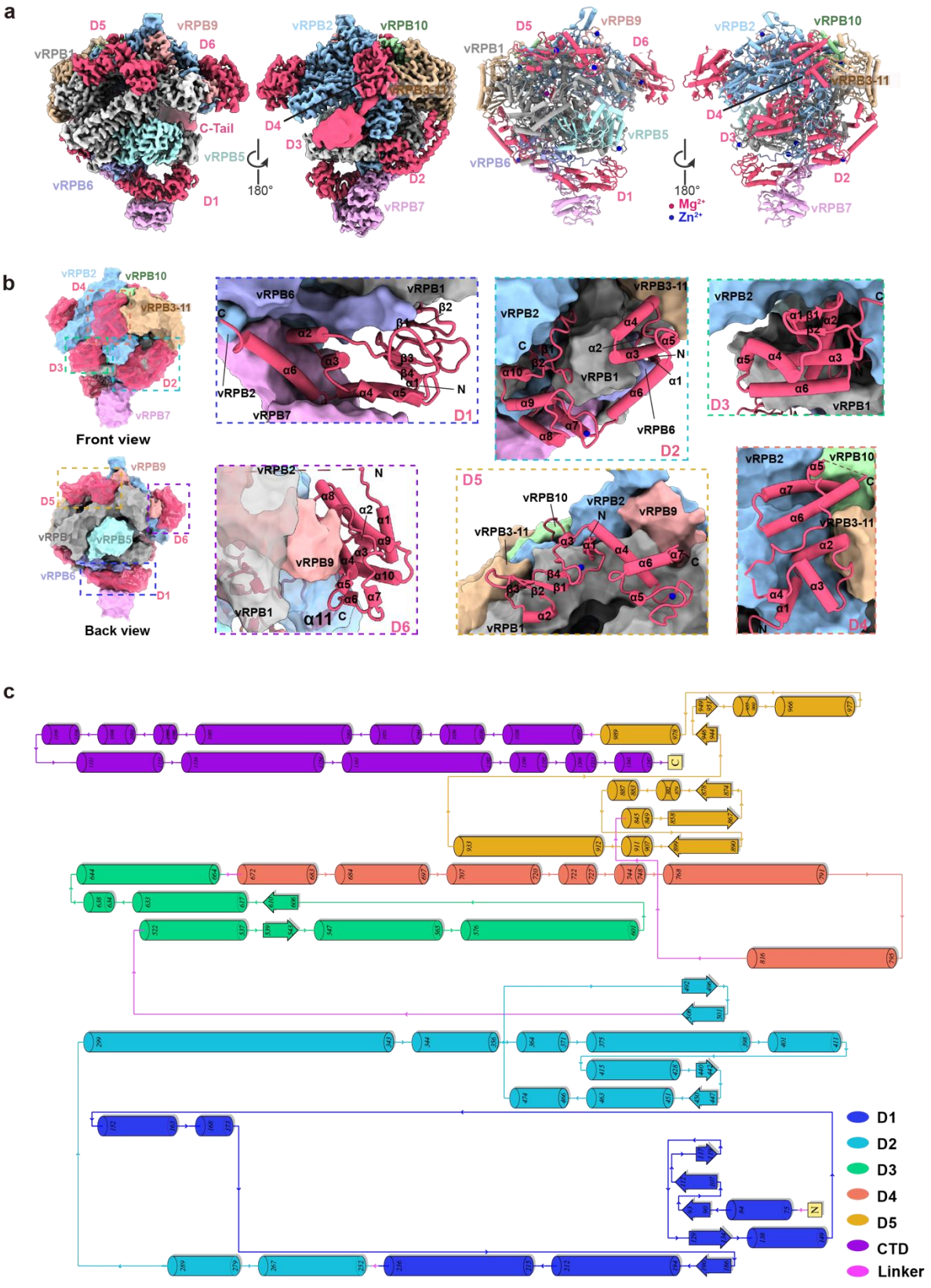

Topology diagrams of the individual domains of M1249L

Supplementary Figure 7: The cryo-EM structures of ASFV vRNAP-M1249L Complex. (**a**) The cryo-EM map (D1:EMD-39509, D2:EMD-39506, D4/D5/D6:EMD-39505) and the structure of the ASFV vRNAP-M1249L complex (PDB:8YQY) shown in two different views rotated by 180°. The map of the M1249L D3 domain was assembled from a higher resolution map (EMD-39510). The protein is shown in cartoon depiction, with helices depicted as cylinders. Subunits are colored as in Fig. 2 (**b**). The active site metal A and bound zinc ions are shown as spheres. (**b**) Cartoon depiction of M1249L domains with structural details shown in close-in view (PDB:8YQY). All the domains of M1249L are colored in pink. The core vRNAP are depicted in schematic surface representation. All subunits are colored as indicated in (**a**). Domain 1 of M1249L features a bipartite structure with a mixed beta-sheet and an alpha-helix-rich lobe. It primarily interacts with the vRPB7 tip and CTD domains, slightly tilting the C-terminal MTase homolog domain. Minor interactions with vRPB1's clamp head and vRPB6's N-tail induce upward movements. Domain 2 contains two subdomains: the N-subdomain, consisting of two four-helix bundles interacting with vRPB1's 'foot' and 'dock', and the C-subdomain, which includes a four-helix bundle coordinating zinc and interacting with vRPB1 and vRPB2. Domain 3 features a five-helix bundle that binds between vRPB1 and vRPB2, existing at only ~1% density maps, suggesting its flexibility. Domain 4 comprises seven alpha-helices, stabilizing vRNAP's structure. Domain 5, linked to D4, surrounds the NTP entry channel and contains a zinc-finger motif that induces movements in vRPB1 and vRPB5. The C-terminal domain (CTD) has an alpha-helix bundle interacting with vRPB9 and a C-linker inducing movement of vRPB2. The final C-tail, containing an unstructured loop and a short helix, is positioned at the reaction center, enacting vital interactions. (**c**) Topological diagram display of M1249L domains from D1 to CTD. The colors of all domains correspond to the dashed boxes in (b).

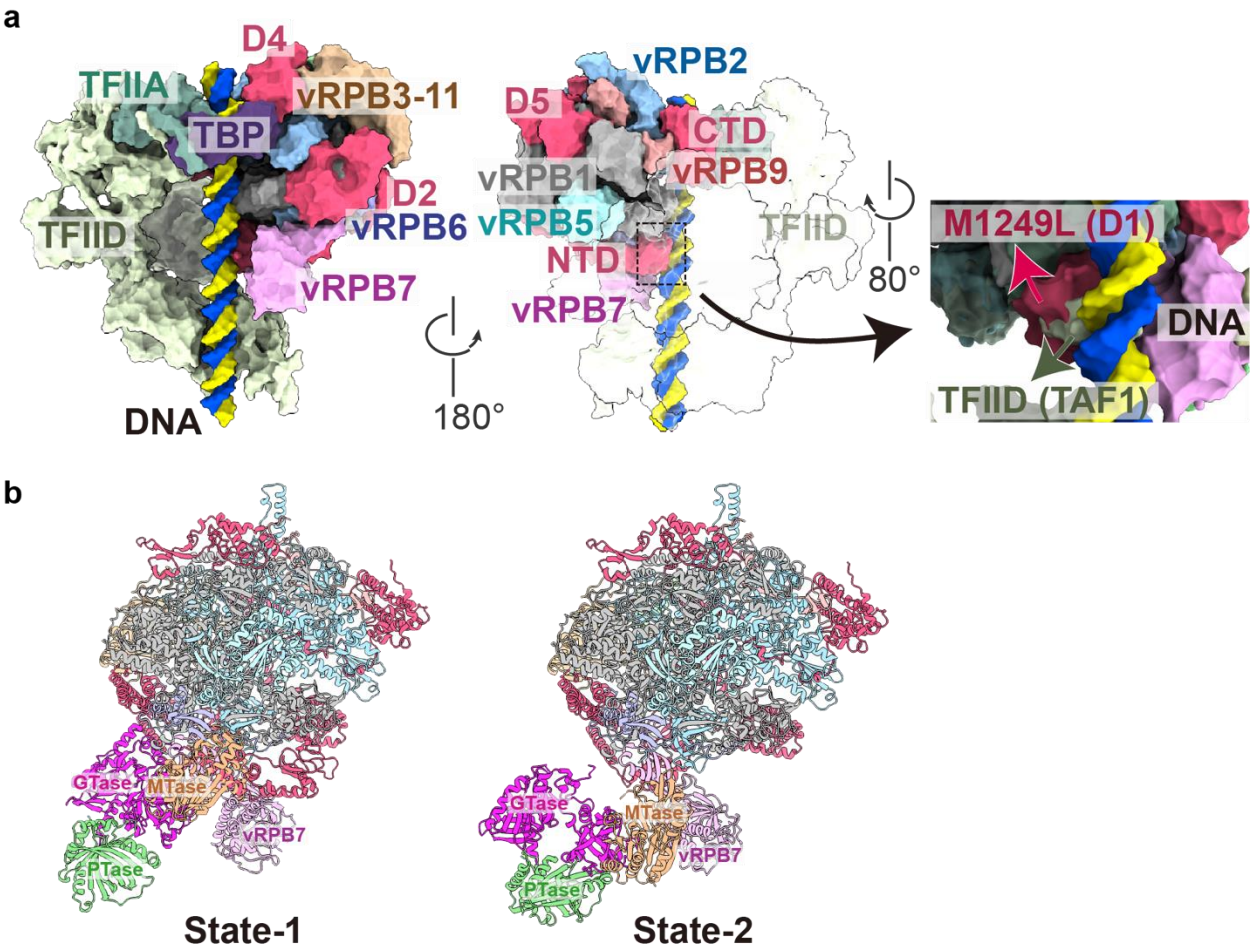

Supplementary Figure 8: D1 of M1249L mimics TAF1 in the preinitiation complex. (**a**) Structural models of ASFV vRNAP superimposed on swine RNAP within the preinitiation complex (PDB: 7EG7), presented from two different views by 180°. The components of vRNAP, DNA, and transcription factors are individually labeled and color-coded. To emphasize the position of D1, TFIID is depicted with heightened transparency. The right panel provides a close-in view comparing D1 and TAF1. (**b**) Structural models of ASFV vRNAP complexed with ASFV capping enzyme (CE). The structures of the functional domains of methyltransferase (MTase), guanylyltransferase (GTase), and triphosphatase (TPase) are predicted using AlphaFold2 and assembled based on the VACV vRNAP structure (PDB: 6RIE). The left panel illustrates a significant clash between MTase and vRPB7, stabilized by D1 of M1249L. The right

panel demonstrates how the absence of D1 allows for a conformational shift in vRPB7, circumventing the clash.

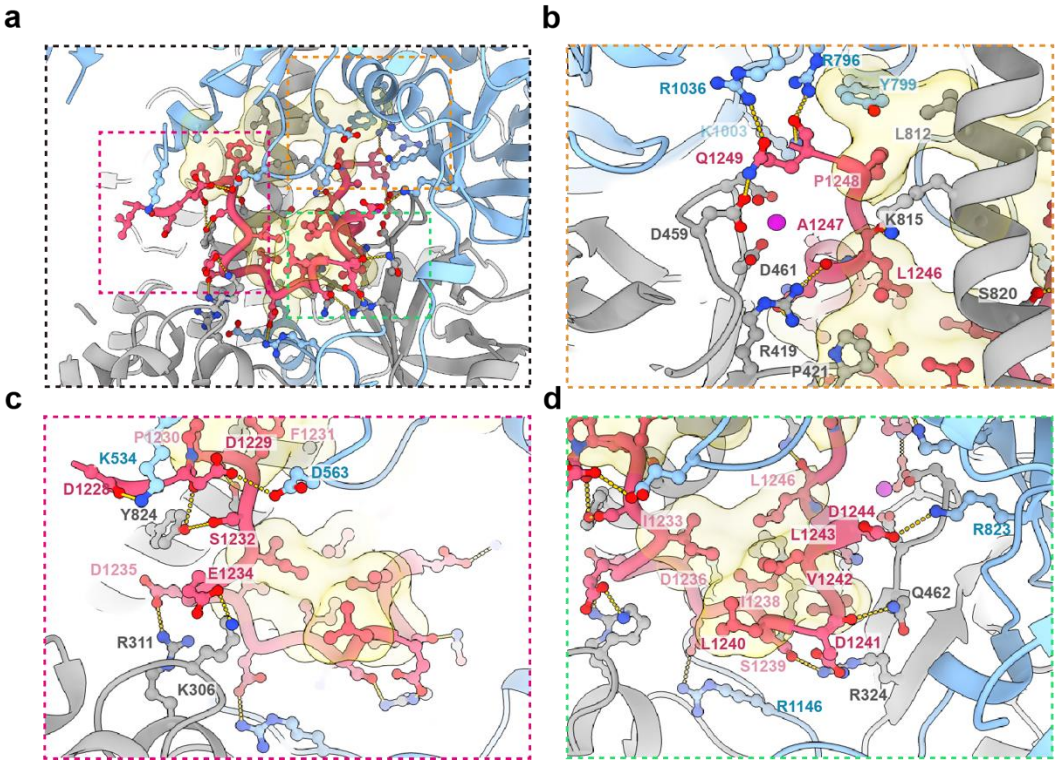

Supplementary Figure 9: Interaction between M1249L C-tail and adjacent vRNAP subunits. (**a**) Overall interaction between M1249L C-tail and adjacent vRNAP subunits. (**b/c/d**) Close-up view of the interaction. ASFV vRNAP subunits are depicted in cartoon, with vRPB1 colored grey and vRPB2 colored blue. Crucial amino acids are highlighted in sphere representation.

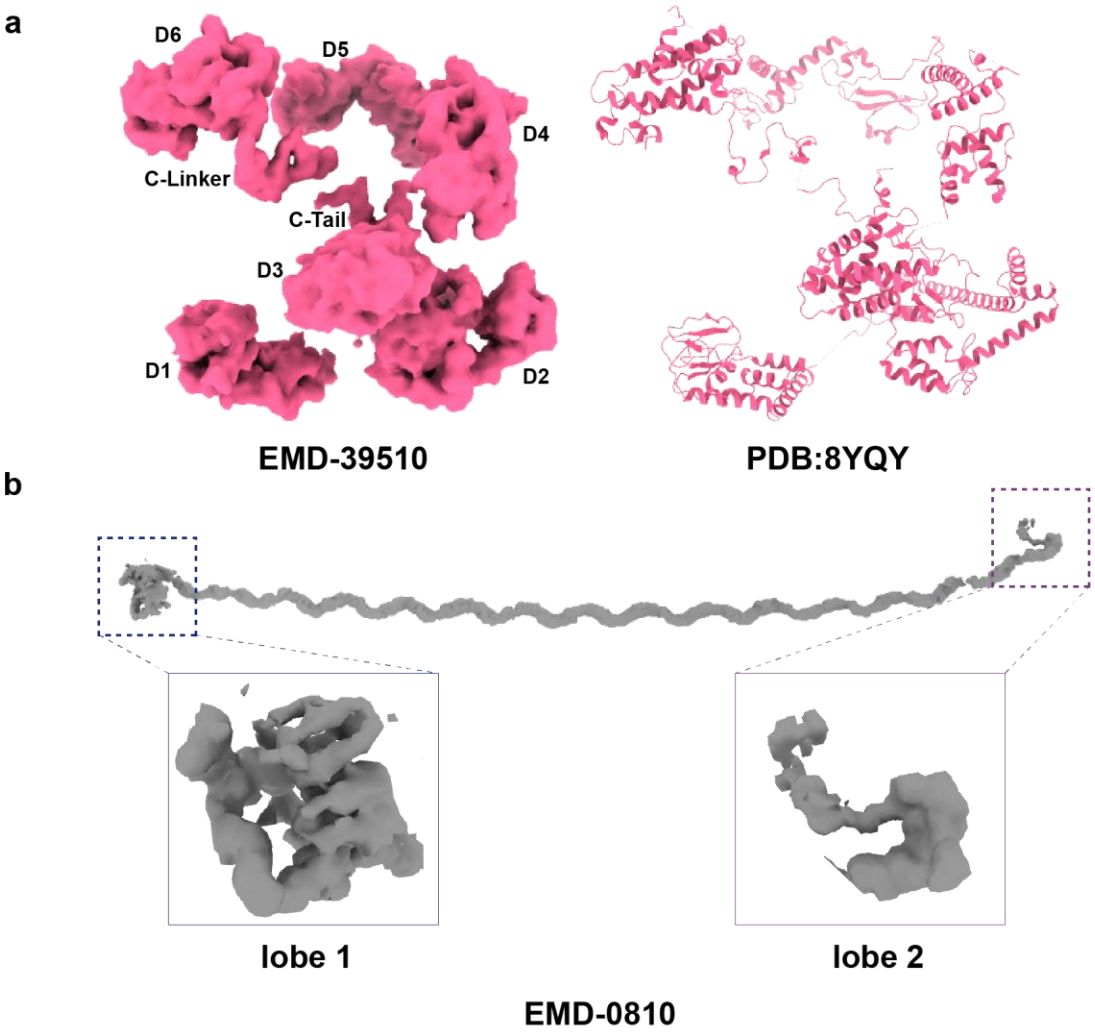

Supplementary Figure 10: Comparation of the two different states of ASFV M1249L. (**a**) The cryo-EM map and the structure of the ASFV M1249L in this paper. (**b**) The cryo-EM map of the ASFV M1249L in virion. Close-up view of the lobe 1 and the lobe 2 of M1249L.

Supplementary Table 1: Statistics for Cryo-EM imaging, data processing and refinement of models

	Core PDB:8YQV	2 PDB:8YQT	4 PDB:8YQX
	Data collection		
EM equipment		FEI Titan Krios	
Voltage (kV)		300	
Detector		Gatan Falcon 4	
Pixel size (Å/pixel)		0.808	
Electron dose ($e^-/Å^2$)		40	
Defocus range (μm)		1-2.5	
Reconstruction			
Number of used particles	354548	475234	218831
Symmetry		C1	
Map sharpening B-factor ($Å^2$)	105.5	101.4	118
Final resolution (Å)	2.67	2.56	2.97
	Model building		
Map CC (mask)	0.84	0.88	0.85
Map CC (peaks)	0.55	0.64	0.48
Map CC (volume)	0.82	0.84	0.8
RMSD (bonds)	0.006	0.004	0.003
RMSD (angles)	0.683	0.593	0.523
	Validation		
MolProbity score	1.76	1.67	1.68
Clash score	9.16	7.45	7.96
	Ramachandran plot		
Outliers	0	0	0
Allowed	3.94	3.19	3.69
Favored	96.06	96.81	96.31
Rotamer outliers	0.36	1.22	0.72
Cβ outliers	0	0.02	0

	3 PDB:8YQW	1 PDB:8YQU	Complete PDB:8YQY
	Data collection		
EM equipment		FEI Titan Krios	
Voltage (kV)		300	
Detector		Gatan Falcon 4	
Pixel size (Å/pixel)		0.808	
Electron dose (e^-/Å^2)		40	
Defocus range (μm)		1-2.5	
Reconstruction			
Number of used particles	218831	61437	10433
Symmetry		C1	
Map sharpening B-factor (Å^2)	95.8	83.4	80.1
Final resolution (Å)	2.68	2.85	3.68
	Model building		
Map CC (mask)	0.88	0.88	0.49
Map CC (peaks)	0.64	0.66	0.54
Map CC (volume)	0.85	0.85	0.54
RMSD (bonds)	0.004	0.003	0.004
RMSD (angles)	0.555	0.552	1.013
	Validation		
MolProbity score	1.6	1.73	1.77
Clash score	6.97	8.44	9.41
	Ramachandran plot		
Outliers	0.02	0	0.06
Allowed	3.36	3.95	3.87
Favored	96.62	96.05	96.07
Rotamer outliers	0.32	0.31	0.27
Cβ outliers	0.02	0.02	0.09

	DNA Complex PDB:8YQZ	5 EMD-39514	6 EMD-39512
	Data collection		
EM equipment	FEI Titan Krios		
Voltage (kV)	300		
Detector	Gatan Falcon 4		
Pixel size (Å/pixel)	0.808		
Electron dose ($e^-/Å^2$)	40		
Defocus range (μm)	1-2.5		
Reconstruction			
Number of used particles	266388	67546	4964
Symmetry	C1		
Map sharpening B-factor (Å2)	104.1	96.9	315.5
Final resolution (Å)	2.78	3.23	9.23
	Model building		
Map CC (mask)	0.86		
Map CC (peaks)	0.7		
Map CC (volume)	0.81		
RMSD (bonds)	0.008		
RMSD (angles)	0.767		
	Validation		
MolProbity score	1.98		
Clash score	7.73		
	Ramachandran plot		
Outliers	0		
Allowed	3.67		
Favored	96.33		
Rotamer outliers	2.55		
Cβ outliers	0		

	7 EMD-39513	8 EMD-39516	9 EMD-39515
	Data collection		
EM equipment	FEI Titan Krios		
Voltage (kV)	300		
Detector	Gatan Falcon 4		
Pixel size (Å/pixel)	0.808		
Electron dose ($e^-/Å^2$)	40		
Defocus range (μm)	1-2.5		
	Reconstruction		
Number of used particles	43341	71418	150008
Symmetry	C1		
Map sharpening B-factor ($Å^2$)	158.8	90.2	95.9
Final resolution (Å)	5.17	3.19	4.04
	Model building		
Map CC (mask)			
Map CC (peaks)			
Map CC (volume)			
RMSD (bonds)			
RMSD (angles)			
	Validation		
MolProbity score			
Clash score			
	Ramachandran plot		
Outliers			
Allowed			
Favored			
Rotamer outliers			
Cβ outliers			

	10 EMD-39517	11 EMD-39518	12 EMD-39519
	Data collection		
EM equipment	FEI Titan Krios		
Voltage (kV)	300		
Detector	Gatan Falcon 4		
Pixel size (Å/pixel)	0.808		
Electron dose ($e^-/Å^2$)	40		
Defocus range (μm)	1-2.5		
	Reconstruction		
Number of used particles	36680	14293	17646
Symmetry	C1		
Map sharpening B-factor ($Å^2$)	75.2	105.2	81.8
Final resolution (Å)	3.49	4.17	3.8
	Model building		
Map CC (mask)			
Map CC (peaks)			
Map CC (volume)			
RMSD (bonds)			
RMSD (angles)			
	Validation		
MolProbity score			
Clash score			
	Ramachandran plot		
Outliers			
Allowed			
Favored			
Rotamer outliers			
Cβ outliers			

	13 EMD-39521	14 EMD-39520	15 EMD-39522
	Data collection		
EM equipment	FEI Titan Krios		
Voltage (kV)	300		
Detector	Gatan Falcon 4		
Pixel size (Å/pixel)	0.808		
Electron dose ($e^-/Å^2$)	40		
Defocus range (μm)	1-2.5		
	Reconstruction		
Number of used particles	1010	16732	5609
Symmetry	C1		
Map sharpening B-factor ($Å^2$)	320	84.5	77.1
Final resolution (Å)	9.32	3.91	4.53
	Model building		
Map CC (mask)			
Map CC (peaks)			
Map CC (volume)			
RMSD (bonds)			
RMSD (angles)			
	Validation		
MolProbity score			
Clash score			
	Ramachandran plot		
Outliers			
Allowed			
Favored			
Rotamer outliers			
Cβ outliers			

	16 EMD-39523	17 EMD-39524	18 EMD-39525
	Data collection		
EM equipment	FEI Titan Krios		
Voltage (kV)	300		
Detector	Gatan Falcon 4		
Pixel size (Å/pixel)	0.808		
Electron dose ($e^-/Å^2$)	40		
Defocus range (μm)	1-2.5		
	Reconstruction		
Number of used particles	20290	42466	53916
Symmetry	C1		
Map sharpening B-factor ($Å^2$)	81.1	90.7	95
Final resolution (Å)	3.59	3.31	3.31
	Model building		
Map CC (mask)			
Map CC (peaks)			
Map CC (volume)			
RMSD (bonds)			
RMSD (angles)			
	Validation		
MolProbity score			
Clash score			
	Ramachandran plot		
Outliers			
Allowed			
Favored			
Rotamer outliers			
Cβ outliers			

	19 EMD-39526	20 EMD-39527	21 EMD-39528
	Data collection		
EM equipment	FEI Titan Krios		
Voltage (kV)	300		
Detector	Gatan Falcon 4		
Pixel size (Å/pixel)	0.808		
Electron dose ($e^-/Å^2$)	40		
Defocus range (μm)	1-2.5		
	Reconstruction		
Number of used particles	15559	17839	24386
Symmetry	C1		
Map sharpening B-factor ($Å^2$)	89.2	91.4	85.5
Final resolution (Å)	4.04	3.86	3.64
	Model building		
Map CC (mask)			
Map CC (peaks)			
Map CC (volume)			
RMSD (bonds)			
RMSD (angles)			
	Validation		
MolProbity score			
Clash score			
	Ramachandran plot		
Outliers			
Allowed			
Favored			
Rotamer outliers			
Cβ outliers			

	22 EMD-39530	23 EMD-39531	24 EMD-39529	25 EMD-39536
		Data collection		
EM equipment			FEI Titan Krios	
Voltage (kV)			300	
Detector			Gatan Falcon 4	
Pixel size (Å/pixel)			0.808	
Electron dose ($e^-/Å^2$)			40	
Defocus range (μm)			1-2.5	
		Reconstruction		
Number of used particles	5431	2338	9630	135954
Symmetry		C1		
Map sharpening B-factor ($Å^2$)	100	92	97.2	84.1
Final resolution (Å)	4.31	6.99	4.04	2.94
		Model building		
Map CC (mask)				
Map CC (peaks)				
Map CC (volume)				
RMSD (bonds)				
RMSD (angles)				
		Validation		
MolProbity score				
Clash score				
		Ramachandran plot		
Outliers				
Allowed				
Favored				
Rotamer outliers				
Cβ outliers				

	M1249L-D1*	M1249L-D2	M1249L-D3
	Model building		
Map CC (mask)	0.72	0.74	0.53
Map CC (peaks)	0.66	0.76	0.74
Map CC (volume)	0.73	0.74	0.53
RMSD (bonds)	0.004	0.004	0.012
RMSD (angles)	1.001	0.979	1.667
	Validation		
MolProbity score	2.16	2.07	0.94
Clash score	13.26	10.23	1.79
	Ramachandran plot		
Outliers	0	0	0
Allowed	9.15	9.69	1.53
Favored	90.85	90.31	98.47
Rotamer outliers	0.68	0	0
Cβ outliers	NA	NA	0.76

	M1249L-D4	M1249L-D5	M1249L-CTD
	Model building		
Map CC (mask)	0.66	0.74	0.73
Map CC (peaks)	0.64	0.68	0.70
Map CC (volume)	0.66	0.74	0.73
RMSD (bonds)	0.008	0.004	0.004
RMSD (angles)	1.252	0.937	0.988
	Validation		
MolProbity score	3.09	1.89	1.61
Clash score	19.60	9.11	5.54
	Ramachandran plot		
Outliers	0	0	0
Allowed	6.5	2.76	4.42
Favored	93.5	97.24	95.58
Rotamer outliers	14.16	2.22	0.48
Cβ outliers	0.81	NA	NA

* All domain structures of the M1249L were validated from the best resolution map (D1, EMD-39509, PDB:8YQX; D2, EMD-39506, PDB:8YQU; D3, EMD-39510, 8YQY; D4/D5/CTD, EMD-39505, PDB:8YQT).

Supplementary Table 2: Summary of models

Subunit Name	Chain	Total residues/ range built	Unmodelled residues	% atomic model
ASFV RNAP Polymerase core				
vRPB1	A	1450/2-212, 224-275, 297-1056, 1073-1132, 1143-1212, 1221-1442	1, 213-223, 276-296, 1057-1072, 1133-1142, 1213-1220, 1443-1450	1375/1450
vRPB2	B	1242/8-217, 225-489, 504-526, 537-940, 949-1242	1-7, 218-224, 490-503, 527-536, 941-948	1196/1242
vRPB3-11	C	359/3-359	45293	357/359
vRPB5	D	205/1-205	-	205/205
vRPB6	E	147/42-147	1-41	106/147
vRPB7	F	339/1-339	-	339/339
vRPB9	G	105/47-105	1-46	59/105
vRPB10	H	80/1-80	-	80/80
ASFV RNAP Polymerase-M1249L Complex Complete				
vRPB1	A	1450/2-211, 225-275, 297-1442	1, 212-224, 276-296,	1407/1450
vRPB2	B	1242/4-218, 225-489, 504-528, 533-940, 949-1242	1-3, 219-224, 490-503, 529-532, 941-948	1207/1242
vRPB3-11	C	359/3-359	45293	357/359
vRPB5	D	205/1-205	-	205/205
vRPB6	E	147/39-147	1-38	109/147
vRPB7	F	335/1-335	-	335/335
vRPB9	G	105/1-105	-	105/105
vRPB10	H	80/1-80	-	80/80
M1249L	J	1249/74-239, 247-729, 734-755, 768-991, 1011-1218, 1227-1249	1-73, 240-246, 730-733, 756-767, 992-1010, 1219-1226	1126/1249

Subunit Name	Chain	Total residues/ range built	Unmodelled residues	% atomic model
ASFV RNAP Polymerase-M1249L Complex 2				
vRPB1	A	1450/1-212, 224-275, 297-1442	213-223, 276-296, 1443-1450	1410/1450
vRPB2	B	1242/4-218, 225-489, 504-527, 535-940, 949-1242	1-3, 219-224, 490-503, 528-534, 941-948	1204/1242
vRPB3-11	C	359/1-359	-	359/359
vRPB5	D	205/1-205	-	205/205
vRPB6	E	147/48-147	1-47	100/147
vRPB7	F	339/1-339	-	339/339
vRPB9	G	105/1-105	-	105/105
vRPB10	H	80/1-80	-	80/80
M1249L	J	1249/672-751, 771-991, 1011-1217, 1227-1249	1-671, 752-770, 992-1010, 1216-1226	531/1249
ASFV RNAP Polymerase-M1249L Complex 1				
vRPB1	A	1450/2-211, 225-275, 297-1442	1, 212-224, 276-296, 1443-1450	1407/1450

vRPB2	B	1242/4-218, 225-489, 504-528, 533-940, 949-1242	1-3, 219-224, 490-503, 529-532, 941-948	1207/1242
vRPB3-11	C	359/3-359	45293	357/359
vRPB5	D	205/1-205	-	205/205
vRPB6	E	147/39-147	1-38	109/147
vRPB7	F	339/1-335	336-339	335/339
vRPB9	G	105/1-105	-	105/105
vRPB10	H	80/1-80	-	80/80
M1249L	J	1249/74-239, 247-517, 672-751, 768-991, 1011-1218, 1227-1249	1-73, 240-246, 518-671, 752-767, 992-1010, 1219-1226	972/1249

Subunit Name	**Chain**	**Total residues/ range built**	**Unmodelled residues**	**% atomic model**
ASFV RNAP Polymerase-M1249L Complex 3				
vRPB1	A	1450/2-211, 225-275, 297-1442	1, 212-224, 276-296, 1443-1450	1407/1450
vRPB2	B	1242/4-218, 225-489, 504-528, 533-940, 949-1242	1-3, 219-224, 490-503, 529-532, 941-948	1207/1242
vRPB3-11	C	359/3-359	1/2	357/359
vRPB5	D	205/1-205	-	205/205
vRPB6	E	147/39-147	1-38	109/147
vRPB7	F	339/1-336	337-339	336/339
vRPB9	G	105/1-105	-	105/105
vRPB10	H	80/1-80	-	80/80
M1249L	J	1249/74-239, 672-751, 768-991, 1011-1218, 1227-1249	1-73, 240-671, 752-767, 992-1010, 1219-1226	701/1249
ASFV RNAP Polymerase-M1249L Complex 4				
vRPB1	A	1450/1-212, 224-275	213-223, 276-1450	264/1450
vRPB7	F	339/1-336	337-339	336/339
M1249L	J	1249/74-239	1-73, 240-1249	166/1249

Supplementary Table 3: Dynamic structures of ASFV RNA polymerase core and its complexes with DNA and M1249L

	EMD	PDB		D1	D2	D3	D4	D5	D6	C-tail	DNA
ASFV RNA polymerase-M1249L complex 24	39529		DNA-Intact	√	√	√	√	√	√		√
ASFV RNA polymerase-M1249L complex 22	39530		DNA-ΔD6	√	√	√	√	√			√
ASFV RNA polymerase-M1249L complex 23	39531		DNA-ΔD5/D6	√	√	√	√				√
ASFV RNA polymerase-M1249L complex 21	39528		DNA-ΔD2/D3	√			√	√	√		√
ASFV RNA polymerase-M1249L complex 20	39527		DNA-ΔD2/D3/D6	√			√	√			√
ASFV RNA polymerase-M1249L complex 17	39524		DNA-ΔD1-D3				√	√	√		√
ASFV RNA polymerase-M1249L complex 19	39526		DNA-ΔD2-D5	√					√		√
ASFV RNA polymerase-M1249L complex 16	39523		DNA-ΔD1-D5						√		√
ASFV RNA polymerase-M1249L complex 18	39525		DNA-ΔD2-D6	√							√
ASFV RNA polymerase-M1249L complex 13	39521		Apo-ΔD6	√	√	√	√	√			
ASFV RNA polymerase-M1249L complex 12	39519		Apo-ΔD2/D3/D5	√			√		√		
ASFV RNA polymerase-M1249L complex 7	39513		Apo-ΔD1-D3/D5				√		√		
ASFV RNA polymerase-M1249L complex11	39518		Apo-ΔD2/D3/D5/D6	√			√				
ASFV RNA polymerase-M1249L complex 5	39514		Apo-ΔD1-D5						√		
ASFV RNA polymerase-M1249L complex 6	39512		Apo-ΔD1-D3/D5/D6				√				
ASFV RNA polymerase-M1249L complex 8	39516		Apo-ΔD2-D6	√							
ASFV RNA polymerase-M1249L complex complete	39510	8YQY	I-Intact	√	√	√	√	√	√	√	
ASFV RNA polymerase-M1249L complex 15	39522		I-ΔD3	√	√		√	√	√	√	
ASFV RNA polymerase-M1249L complex 14	39520		I-ΔD3/D4	√	√			√	√	√	
ASFV RNA polymerase-M1249L complex10	39517		I-ΔD2-D4	√				√	√	√	
ASFV RNA polymerase-M1249L complex25	39536		I-ΔD1-D4					√	√	√	
ASFV RNA polymerase-M1249L complex 9	39515		I-ΔD2-D5	√					√	√	
ASFV RNA polymerase-M1249L complex2	39505	8YQT	I-ΔD1-D3				√	√	√	√	
ASFV RNA polymerase-DNA complex	39511	8YQZ									√
ASFV RNA polymerase-M1249L complex4	39509	8YQX		√							
ASFV RNA polymerase-M1249L complex3	39508	8YQW		√			√	√	√	√	

ASFV RNA polymerase core	39507	8YQV									
ASFV RNA polymerase-M1249L complex1	39506	8YQU		√	√		√	√	√	√	